Investigation of Active Flow Control Using a Differential Reynolds Stress Model

V. Togiti, V. Ciobaca, and B. Eisfeld

Abstract. In the present work the predictive capabilities of different turbulence models for active flow control applications by means of vortex generator jets are evaluated by comparing numerical predictions with experimental data. With suitable turbulence model, the influence of orientation of actuator and jet velocity ratio are studied for a round jet actuator on a flat plate with zero pressure gradient. Finally, a two-element high-lift airfoil with a pair of vortex generator jets on the leading-edge of the main wing is studied with an emphasis on the interaction of longitudinal vortices with boundary layer under adverse pressure gradient.

1 Introduction

Flow separation on aerodynamic surfaces leads to decreased lift and increased drag. To improve aerodynamic performance, the separation has to be delayed or avoided. This is done by controlling the flow either actively or passively which brings higher momentum very close to wall. In passive flow control, the flow field is modified through stationary devices such as vortex generators. Passive flow control devices can increase the drag even when flow does not separate. Due to this drawback, active flow control technique has become prominent over the past decades, in which time-dependent or constant disturbances are introduced into the flow field by actuator devices. In active flow control, the intent is to apply the control device when needed, thus it does not affect performance when it is not applied.

V. Togiti · B. Eisfeld
German Aerospace Center (DLR), Institute of Aerodynamics and Flow Technology,
Department $C^2A^2S^2E$, Braunschweig, Germany
e-mail: {vamshi.togiti,bernhard.eisfeld}@dlr.de

V. Ciobaca
German Aerospace Center (DLR), Institute of Aerodynamics and Flow Technology,
Department TF, Braunschweig, Germany
e-mail: vlad.ciobaca@dlr.de

A. Dillmann et al. (Eds.): *New Results in Numer. & Exp. Fluid Mech.*, NNFM 121, pp. 161–168.
DOI: 10.1007/978-3-642-35680-3_20

In the past, most of the experimental studies were pertaining to shape, orientation and direction of the actuator which would increase mixing in the boundary layer and enhance momentum in the vicinity of wall but not much about the fundamental mechanism. For investigating active flow control mechanism, numerical simulations are useful. As the flow interaction is complex, numerical predictions often depend upon the turbulence model employed.

Large-eddy simulation (LES) is generally used to study active flow control mechanism. Due to very high computational effort required for LES, the Reynolds averaged Navier-Stokes (RANS) approach with eddy viscosity models (EVM) is often employed for industrial applications. These models predict attached boundary layers fairly well, but are observed to fail in case of separation and very often dissipate free vortices rapidly. This can be attributed to the production terms of underlying transport equations which need modeling. In contrast to eddy viscosity models, differential Reynolds stress models (RSM) provide individual transport equations for the Reynolds stresses and the production terms in the transport equations are exact.

Therefore, the present investigation deals with evaluating the predictive capabilities of different RANS turbulence models for a flat plate with continuously blowing round jet actuator and demonstrating the RSM superiority over EVM. In detail, first, the RSM and EVM are applied to a flat plate with continuously blowing round jet actuator to demonstrate superiority. Secondly, the RSM is applied to the flat plate with continuously blowing actuator to study the influence of actuator orientation and jet velocity ratio on flow control mechanism. Finally, a two-element high-lift airfoil with a pair of vortex generator jets on the leading edge of the main wing is investigated using the RSM focusing on the interaction of longitudinal vortices with the boundary layer under adverse pressure gradient.

2 Test Case and Numerical Methodology

The configurations investigated are based on the experimental work carried out within the German national project M-Fly [6] at the Technical university Braunschweig for the flat plate and in the low-speed facility (DNW/NWB) at DLR for a two-element high lift airfoil (FNG). In the case of flat plate experiment, a flat plate with continuously blowing actuator located at $L = 53\delta_l$ downstream of the leading-edge is studied at a Reynolds number $Re_L = 7.76 \times 10^6$ and jet velocity ratios $\frac{U_{jet}}{U_\infty} = 2.5$ and 5.0. Here δ_l is the boundary layer thickness at the actuator position. In the two-element high lift experiment, a segment $(\Delta y/c = 0.05)$ of full span of model equipped with a pair of convergent actuators with skew angle of 90° and pitch angle of 30° located at $x/c = 0.01$ on the lower side of the wing is investigated at Reynolds number of 2×10^6, Mach number of 0.15 and jet velocity ratio of 6.6.

In this study the TAU Code [3] is used, which is the compressible flow solver developed at DLR and is based on an unstructured finite volume scheme. In the current investigation viscous fluxes are discretized using central differences, inviscid fluxes are calculated by a central method with matrix dissipation and steady computations are performed using a semi-implicit lower-upper symmetric Gauss-

Seidel (LU-SGS) method. In the current study, for both configurations, hybrid grids generated using the MegaCads are used. In these studies the grids with spanwise width of $(\Delta y/\delta_l)$ 14.7 and $(\Delta y/c)$ 0.05 for the flat plate and the FNG are considered, respectively. The grids used in the study are based on the grid refinement studies performed in [5]. In the present investigation a portion of the actuator is modeled and for the actuator wall Euler wall condition and at the inlet of the actuator maximum jet velocity and density are prescribed.

3 Turbulence Model Study

To evaluate predictive capabilities of different RANS turbulence models for active flow control, the one-equation Spalart-Allmaras model (SA) [4], the shear stress transport (SST) $k-\omega$ model [2] and the SSG/LRR-ω Reynolds stress model [1] are applied to a flat plate with circular injector at pitch angle $\alpha = 45^\circ$, skew angle $\beta = 90^\circ$ and jet velocity ratio $\lambda = 2.5$.

In Fig. 1, streamlines on planes extracted at two different locations downstream of the injector are shown. These streamlines render vortices generated due to actuation. From these figures it can be observed that, with all the applied models the primary vortex size increases along with the downstream distance. At $x/\delta_l = 0.6$ the SST and the SSG/LRR-ω model both predict a fairly strong secondary vortex, while this is not well captured with the SA model. At the afore mentioned location the SSG/LRR-ω model predicts a small tertiary vortex which is not visible in the predictions with the other models. Further downstream of this location, at $x/\delta_l = 1.2$ the secondary vortex has dissipated with the SA model while with the SST and the SSG/LRR-ω model it is still kept.

Contours of the streamwise velocity delivered by different turbulent models at $x/\delta_l = 2.4$ downstream of the injector are shown in the first column of Fig. 2 and compared with the measurements. It is apparent from these contours that the

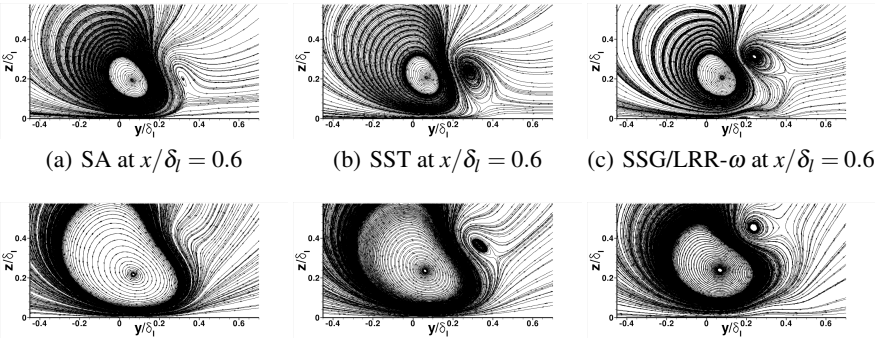

(a) SA at $x/\delta_l = 0.6$ (b) SST at $x/\delta_l = 0.6$ (c) SSG/LRR-ω at $x/\delta_l = 0.6$

(d) SA at $x/\delta_l = 1.2$ (e) SST at $x/\delta_l = 1.2$ (f) SSG/LRR-ω at $x/\delta_l = 1.2$

Fig. 1 Streamlines delivered by different turbulence models at different locations downstream of the injector

strength of the vortex is dissipated too much with the SA and the SST model. In contrast, with the SSG/LRR-ω model the local peak values are retained, and the velocity contours are in good agreement with the measurements.

In Fig. 2 contours of the wall-normal velocity at $x/\delta_l = 2.4$ are depicted and compared with the experiment (figures in the second column). In the experiments local peak values are apparently very close to the wall, representing an anti-clockwise rotating vortex. The predictions show that the contours produced by the SA model and the SST model do not show such peak values as in the experiment, implying that the predicted vortex is not as strong as in the experiment, whereas with the SSG/LRR-ω model the contour levels are in good agreement with the measurements.

Contours of the spanwise velocity downstream of the injector at $x/\delta_l = 2.4$ are displayed in the third column of Fig. 2 and compared with the experiment. The contours in the experiment show a high local velocity close to the wall indicating a vortex. This trend is reproduced with all of the turbulence models. However the level of the peak values is underpredicted with the SA and SST models, while almost the same level as in the experiment is predicted with the SSG/LRR-ω model.

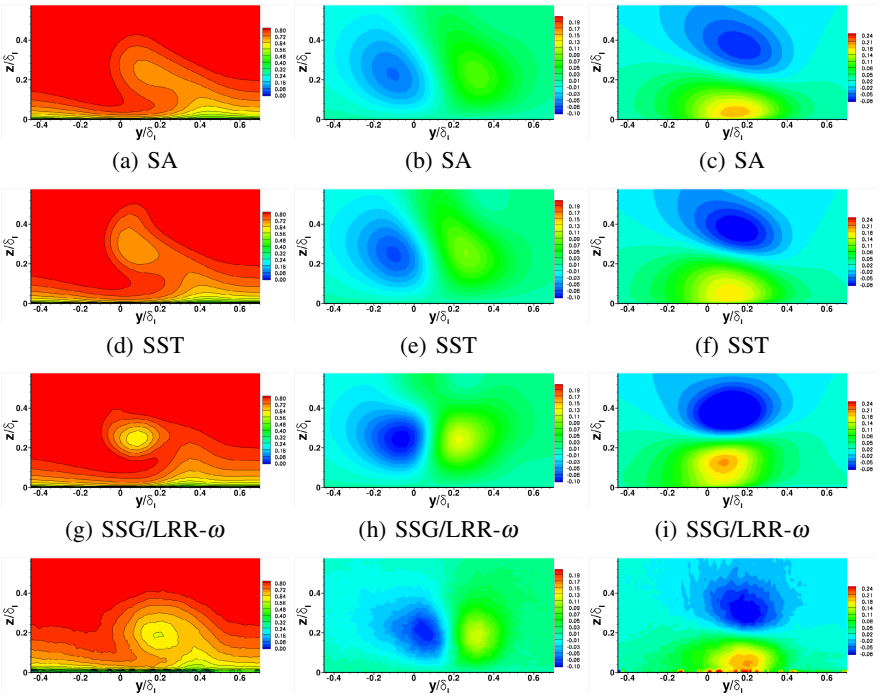

Fig. 2 Contours of non-dimensional velocity at $x/\delta_l = 2.4$ downstream of the injector for different turbulence models: Streamwise velocity contours are shown in the first column. In the second and third column wall-normal and spanwise velocity contours are shown, respectively

As can be seen in the Fig. 2 the SA and the SST models are able to reproduce the trends of the experiment, but they are unable to keep the vortex strength farther downstream. In contrast, with the SSG/LRR-ω model it is possible to predict a tertiary vortex close to the wall and also to reproduce experiments more accurately farther downstream. This can be attributed to the exact treatment of the production term in differential Reynolds stress models.

4 Investigation of Influence of Injector Orientation and Jet Velocity Ratio

Here, the effectiveness of actuation is studied using the SSG/LRR-ω model. For this purpose, actuators orientation and jet velocity ratio have been varied. In the case of orientation studies, the actuators with pitch angles $\alpha = 30^\circ$ and $\alpha = 45^\circ$ and skew angle $\beta = 90^\circ$ at jet velocity ratio $\lambda = 2.5$ are simulated. In jet velocity ratio studies, the jet velocity ratio is raised from 2.5 to 5.0 at pitch angle of 30° and skew angle of 90°.

Profiles of the momentum coefficient ΔR_{vx} downstream of the injector for different pitch angles and jet velocity ratios are shown in Fig. 3 and compared with the measurements. The momentum coefficient is defined as given in Equation (1). Here u and u_0 are disturbed and undisturbed velocities, respectively.

$$\Delta R_{vx} = \frac{\int_{y_1}^{y_2} (u^2 - u_0^2)\, dy}{\int_{y_1}^{y_2} u_0^2\, dy} \tag{1}$$

In boundary layer, a positive and a negative sign for ΔR_{vx} render gain and loss of momentum due to actuation, respectively. In the experiments a higher momentum coefficient is apparent close to the wall when the pitch angle reduced from 45° to 30° at the jet velocity ratio of 2.5. This trend is well reproduced in the numerics. In Fig. 3(a), the momentum coefficient profiles for two different pitch angles deviate from the measurements above the wall which is due to a secondary vortex observed in the simulations. When the jet velocity ratio increased from 2.5 to 5.0, a higher momentum coefficient close to the wall can be seen in the experiment at the pitch angle of 30°. Overall, the predictions delivered by the SSG/LRR-ω not only follow the experimental trends but also agree well with the measurements.

From the perspective of flow control, it is essential to bring high momentum fluid into the near-wall regions so that the resulting boundary layer can sustain to adverse pressure gradient and separation can be avoided. From the measurements and predictions it is apparent that high momentum fluid can be brought into near-wall region by decreasing skew angle and increasing jet velocity ratio.

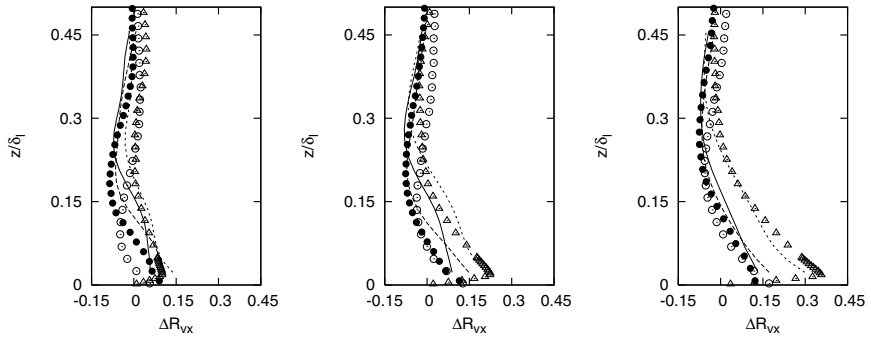

(a) $x/\delta_l = 1.2$ (b) $x/\delta_l = 2.4$ (c) $x/\delta_l = 4.8$

Fig. 3 Momentum coefficient profiles downstream of the injector; Lines: predictions, symbols: experiment. ●, ———: $\alpha = 45°, \beta = 90°$ and $\lambda = 2.5$. ⊙, – – – – –: $\alpha = 30°, \beta = 90°$ and $\lambda = 2.5$. △, - - - - - - : $\alpha = 30°, \beta = 90°$ and $\lambda = 5.0$.

5 Investigation of a Two-Element Airfoil with Vortex Generator Jets

In the current investigation a two-element high-lift airfoil equipped with two convergent actuators with pitch angle $\alpha = 30°$ and skew angle $\beta = 90°$ located on the lower side of the wing at $x/c = 0.01$, in between leading-edge and stagnation point, is simulated with the SSG/LRR-ω RSM. In this study the incidence in the linear region of the polar, 5° to 7.5°, at Reynolds number $Re_c = 2 \times 10^6$, Mach number $Ma = 0.14$ and jet velocity ratio $\lambda = 6.6$ are investigated.

In Fig.4, pressure coefficient distribution along the main wing and flap at various incidence is illustrated. Overall, the predicted pressure distribution is in good agreement with the measurements. However, discrepancies persist at the leading-edge and on the suction side of the flap. The predictions show larger separation extent on the flap compare to the experiment.

Spanwise variation of pressure coefficient on the suction side of the main wing at x/c = 0.01 is depicted in Fig. 4(c) for the incidence 5° and 7°. In the measurements a zigzag pattern can be observed. This is due to presence of longitudinal vortices. As the angle of attack increases, the pattern becomes much prominent in the experiment. Similar to the measurements, spanwise varying pressure distribution can be observed in the numerical predictions. However, the predicted levels are slightly different from the measurements.

Contours of non-dimensional streamwise velocity difference ΔU at three different locations downstream of the injector on the suction side of the main wing are shown in Fig. 5. Here, ΔU is the velocity difference between the boundary layer with and without active flow control (AFC) $(U_{withAFC} - U_{withoutAFC})$. A positive and a negative value of ΔU render velocity gain and loss, respectively. In the figures, at any given incidence velocity loss and velocity gain are apparent which are due to vortex roll-up and vortex roll-down, respectively. In the Fig. 5 it is evident that the

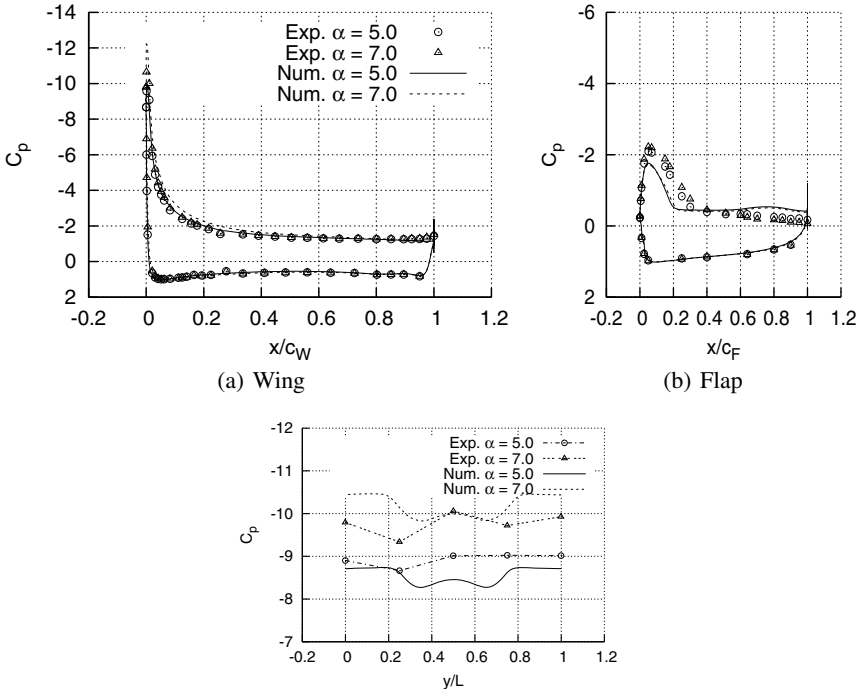

(a) Wing (b) Flap

(c) Spanwise Cp at $x/c = 0.01$

Fig. 4 C_p distribution along wing, flap at various angles of attack

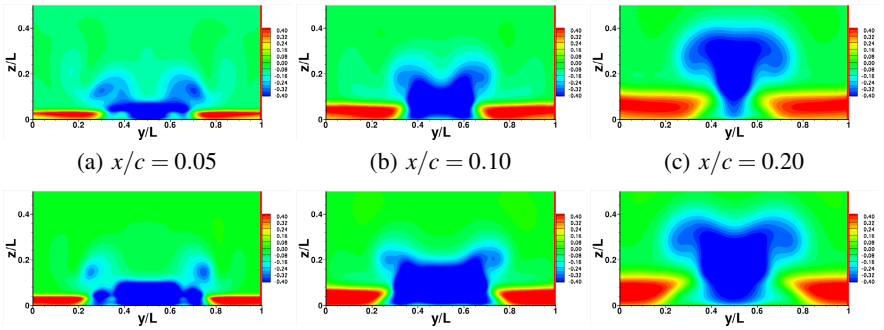

(a) $x/c = 0.05$ (b) $x/c = 0.10$ (c) $x/c = 0.20$

(d) $x/c = 0.05$ (e) $x/c = 0.10$ (f) $x/c = 0.20$

Fig. 5 Contours of non-dimensional streamwise velocity difference, $\frac{\Delta U}{U_{ref}}$, at different locations downstream of the injector. (a)-(c): $\alpha = 5.0^\circ$ and (d)-(f): $\alpha = 7.5^\circ$

extent of velocity loss close to wall $(z/L \approx 0)$ decreases as the flow moves downstream. Similar trend can be observed for the other angle of attack. In the figures the extent of blockage is shown by velocity loss which increases with incidence.

6 Summary

In the present work, numerical studies were performed for active flow control by means of vortex generator jets on a flat plate with zero pressure gradient and a two-element high-lift airfoil (FNG). The investigations regarding the flat plate studies were pertaining to suitable turbulence models and the influence of the orientation of actuator and jet velocity ratio on the flow control mechanisms. Regarding the FNG, the studies were concerning investigating the interaction of multiple longitudinal vortices with the boundary layer under adverse pressure gradinet.

Turbulence model study for the flat plate revealed that the SA and the Menter SST models are unable to keep the vortices farther downstream of the injector. In contrast, the predictions by the SSG/LRR-ω model not only follow the experimental trends, but also agree well with the measurements quantitatively. Henceforth, the SSG/LRR-ω model was applied for the further investigations.

The influences of pitch angle and jet velocity ratio on the flow control mechanism were studied on a flat plate with circular actuator. When the pitch angle changed from 45° to 30° at the skew angle of 90° and jet velocity ratio of 2.5, higher momentum coefficient in the near wall region was observed. Similar trend was also noticed when the jet velocity ratio increased from 2.5 to 5.0. All the observed trends were in line with the experimental findings.

The interaction of longitudinal vortices with boundary layer was studied for the FNG airfoil in the linear regime of the polar. The predictions showed velocity gain in the near-wall region due to vortex roll-down. The extent of the velocity gain increases with the downstream distance. However, with incidence the extent decreases due to blockage effect of the counter-rotating vortices.

References

1. Eisfeld, B., Brodersen, O.: Advanced Turbulence Modelling and Stress Analysis for the DLR-F6 Configuration. AIAA-Paper 2005-4727 (2005)
2. Menter, F.R.: Two-Equation Eddy-Viscosity Turbulence Models for Engineering Applications. AIAA Journal 32(8), 1598–1605 (1994)
3. Schwamborn, D., Gerhold, T., Heinrich, R.: The DLR TAU-Code: Recent Applications in Research and Industry. In: European Conf. on CFD, ECCOMAS CFD (2006)
4. Spalart, P.R., Allmaras, S.R.: A One-Equation Turbulence Model for Aerodynamic Flows. La Recherche Aerospatiale 1, 5–21 (1994)
5. Togiti, V., Ciobaca, V., Eisfeld, B.: Numerical Simulation of Steady Blowing Active Flow Control using a Differential Reynols Stress model. In: CEAS/KATnet II Conference, Bremen, Germany, May 12-14 (2009)
6. Wild, J., Wichmann, G., Haucke, F., Peltzer, I., Scholz, P.: Large scale separation flow control experiments within the German Flow Control Network. AIAA-Paper 2009-530 (2009)